



Synthesis of bactericidal polymer coatings by sequential plasma-induced polymerization of 4-vinyl pyridine and gas-phase quaternization of poly-4-vinyl pyridine

Martha Hernández-Orta¹ , Elías Pérez² , Luis Emilio Cruz-Barba³ , and Marco A. Sánchez-Castillo^{1,4,*} 

¹ Facultad de Ciencias Químicas, Universidad Autónoma de San Luis Potosí, Manuel Nava 6, 78210 San Luis Potosí, S.L.P., Mexico

² Instituto de Física, Universidad Autónoma de San Luis Potosí, Manuel Nava 6, 78210 San Luis Potosí, S.L.P., Mexico

³ Departamento de Ingeniería Química-CUCEI, Universidad de Guadalajara, Marcelino García Barragán 1421, 44430 Guadalajara, Jal, Mexico

⁴ Coordinación para la Innovación y la Aplicación de la Ciencia y la Tecnología, Universidad Autónoma de San Luis Potosí, Sierra Leona 550, 78210 San Luis Potosí, S.L.P., Mexico

Received: 24 October 2017

Accepted: 27 February 2018

Published online:

12 March 2018

© Springer Science+Business Media, LLC, part of Springer Nature 2018

ABSTRACT

Plasma-based technology is an alternative to produce universal polymer coatings with the appropriate requirements of robustness and stability for antibacterial applications. Here, we proposed a sequential two-step alternative to synthesize antibacterial polymer coatings. A non-isothermal plasma reactor, operated at atmospheric pressure (P_{atm}) and room temperature (T_{room}), was used to induce free radical polymerization of 4-vinyl pyridine (4VP) on high-density polyethylene (PE). In a subsequent step, the poly-4VP (P4VP) films were treated with a bromoethane/He gas stream to produce quaternized P4VP (P4VPQ) films. Chemical structure of polymer films was validated by infrared and UV–visible spectroscopy, and morphology was evaluated by optical and atomic force microscopy; scanning electron microscopy was used to determine films thickness, which was then used to estimate the surface charge density. The bactericidal capacity was determined with a standard test by using *Escherichia coli*. Both types of films had an estimated charge density in the order of 10^{16} positive charges per cm^2 ; P4VP films removed about 95–99% of bacteria, whereas P4VPQ films eliminated 100%. The methodology proposed for the synthesis of antibacterial polymer coatings is simpler, faster, and more environmentally friendly than other plasma-based methods; operation at T_{room} and P_{atm} may also have a significant effect on the economics and the ease of implementation of the process at commercial scale. The suggested approach may facilitate the development of new universal coatings, and operating plasma conditions could be extrapolated for engineering antibacterial coatings in industrial areas where bacterial attachment is of concern.

Address correspondence to E-mail: masanchez@uaslp.mx

Introduction

Bacterial adhesion on biotic and abiotic surfaces is a major problem in health care, food packaging, and industrial and marine biofouling, with significant technical and economic consequences [1, 2]. In particular, the development of nosocomial infections, mostly attributed to Gram-negative bacterial pathogens, is considered a major health challenge in healthcare units worldwide [3]. One alternative to control risk factors for nosocomial infections is the development of antibacterial coatings whose performance could be improved by the presence of additional antibacterial agents [1, 3]. Many research studies have been focused to develop antibacterial surfaces and thin coatings that can be applied to different supports such as hydrogels, ceramics, and plasma-deposited polymers. More recently, the emphasis is oriented to the development of universal polymer coatings, which are substrate independent [1, 3, 4]. To accomplish this purpose, a dense surface coating should be obtained to improve the density of the active sites, and additional intra-layer interactions (i.e., physical and chemical cross-linking) should be promoted to enhance the coating's stability. Current universal polymer coating systems include, among others, surface irradiation, layer-by-layer assembly, spin coating, chemical vapor deposition, and laser deposition [4]. Different irradiation methods including plasma, ultraviolet (UV), gamma rays, microwaves, lasers, and electron beams are used to modify the materials' surface and to introduce chemical surface groups [2, 4].

Plasma exposure is rapidly becoming one of the best options to produce functional, non-fouling, and nanocomposite coatings with the appropriate requirements of robustness and long-term stability for antibacterial applications [1, 3]. Plasma modifying strategies include (a) single-step processes: plasma treatment, plasma polymerization, and plasma syn-irradiation, and (b) dual step processes: plasma post-irradiation grafting (PPIG); these methods are described elsewhere in the literature [1, 2, 5]. It should also be noticed that pulsed plasma with short on-periods and long off-periods leads to polymer films with a higher degree of molecular specificity [4]. In the case of PPIG, in a first step, the surface has to be activated and functionalized with a plasma treatment. In a second step, the induced surface

functionalities can subsequently be employed for the initiation of a polymerization reaction, by bringing the surface in contact with monomers in the gas or liquid phase. Since the monomer is not subjected to the plasma condition, the grafted polymer will have the same composition as polymers obtained by conventional polymerization processes [2, 5]. Compared to traditional chemical "wet" methods, plasma-based techniques have some advantages for the fabrication of antibacterial films [1–3, 6, 7]: (a) the ability to modify thin surface layers of conventional materials with no alteration of the bulk, (b) continuous, homogeneous, and pinhole-free coatings, (c) dry technology with no use of solvents (gas-phase dry processes), (d) reduced and effective use of chemicals that promotes economic and environmental benefits, (e) great versatility: applicability to a broad range of substrates and complex-shaped structures, facilitating the development of universal polymer coatings, (f) relatively easy integration in industrial processes.

The mechanism of antibacterial action of polymer coatings is not yet fully elucidated [8]. One of the most widely accepted mechanisms proposes that the loss of activity of a Gram-negative bacterium is due to the effect of positively charged quaternary ammonium compounds [9, 10]. These polymeric structures displace divalent cations (e.g., Ca^{2+} and Mg^{2+}) that keep bacteria attached to their negatively charged lipopolysaccharide network surface; electrical attraction alters the outer membrane of Gram-negative bacteria, such as *Escherichia coli*. Therefore, several coatings are based on the development of surface cationic groups capable of destabilizing the bacterial membrane [9]. In this class of coatings, a number of studies indicate that a positively charged polymer coating is not enough to inactivate or kill the bacteria, but that alkylation of the polymer film to produce surface quaternary ammonium compounds (QAC) is required [7, 9, 11, 12]. To this purpose, the use of pyridinium-type quaternary ammonium salts has been widely suggested because of their broad spectrum of antibacterial activity, high kill rate, and nontoxicity toward mammalian cells [9, 11–13]. It must be noticed that several other methodologies recently used to develop antibacterial coatings can be reviewed elsewhere in the literature [3, 4, 6].

Several two-step approaches have been suggested to develop quaternized polymer coatings with antibacterial coatings by using a wide variety of plasma sources, plasma reaction configurations, and

plasma operating conditions. In general, in a first step, the polymer coating is formed on a given support using some of the indicated plasma-based strategies. In a second step, the quaternization of the polymer coating is made by using pyridinium-type quaternary ammonium salts. For instance, Jampala et al. [11] develop antibacterial surfaces on stainless steel (SS) and filter paper by using non equilibrium, low-pressure ethylenediamine plasma; the polymer films were covalently attached to the SS via intermediate layer deposited in O_2 and hexamethyldisiloxane plasma. All plasma treatments were made in a parallel-plate plasma reactor by using a 13.6-MHz radio frequency power source. The quaternary ammonium groups were generated by a subsequent ex situ reaction with hexyl bromide and further methylated in methyl iodide. The modified surfaces exhibited antibacterial properties for *Staphylococcus aureus* and *Klebsiella pneumoniae*. In the other hand, Schofield and Badyal [12] showed that a 4-vinyl pyridine polymer film quaternized with bromobutane led to antibacterial films. In the first step, the authors used a low-pressure pulsed-plasma reactor, attached to a 13.56-MHz radio frequency power supply, to promote the polymerization of the vinyl carbon-carbon double bond contained in the 4-vinyl pyridine monomer (retention of the pyridine ring aromatic functionality). In the second step, the pyridine-functionalized surfaces were immersed into a 10% (v/v) solution of bromobutane, keeping the reaction mixture under reflux at 70 °C for periods of up to 8 h. A final stage of preparation comprised rinsing in methanol and distilled water prior to air-drying. The authors reported that the pyridine-functionalized polymer coating was bactericidal toward *Staphylococcus aureus* and *Klebsiella pneumoniae*.

In the indicated experimental procedures, the first step is typically accomplished by using low-pressure plasma to form the polymer coating, either by plasma polymerization or by plasma syn-radiation approaches. In the second step, an ex situ wet process is used to achieve the quaternization of the polymer coating. In this work, we propose an alternative procedure to synthesize antibacterial polymer coatings. In the first step, we propose a plasma post-irradiation grafting approach to form a poly-4-vinyl pyridine (P4VP) coating. To this purpose, a parallel-plate dielectric barrier discharge reactor (DBD-R), operated at room temperature (T_{room}) and atmospheric pressure (P_{atm}), is used to induce the

polymerization of 4-vinyl pyridine (4VP) on high-density polyethylene (PE). In a sequential step, using the same reactor, we induce the quaternization of P4VP with a gas stream of bromoethane/He at T_{room} and P_{atm} to produce positively charged quaternary ammonium films (P-4VPQ). The chemical characterization of the polymeric films is done by infrared spectroscopy (in the ATR mode) and by UV-visible spectroscopy. The morphological characterization of the films is performed by optical and atomic force microscopy. In addition, the bactericidal potential of the polymeric films, before and after the quaternization step, is evaluated using a Gram-negative bacterium (*Escherichia coli*).

Methodology

Materials

High-density polyethylene (PE) was used as substrate for the synthesis of bactericidal films, because it has a simple chemical structure and suitable morphology for the formation of surface polymeric films. A commercial PE sample of 0.6 mm thickness was used. Prior to each treatment, PE surface was washed with 2% Extran[®]; then, it was rinsed with deionized water, and finally, it was dried with an air flow. On the other hand, 4-VP (Sigma Aldrich, 95% purity) was used as monomer. The gases used in NIPT were extra dry oxygen (Praxair, 99.5% purity) and helium (Praxair, 99.996% purity).

Surface treatment system

Figure 1 shows a schematic representation of the non-isothermal plasma treatment (NIPT) used for the synthesis of P4VP and P4VPQ films. The non-isothermal plasma system was built in the laboratory, and it has the following main sections. (a) A feed system, which regulates the mass flow rate of the gases flowing into the reactor by using a multi-channel mass flow controller (MKS) and mass flow meters (MKS). Two glass saturators were set in the system, and one of them contained 4VP, which was used to saturate the He stream flowing to the reactor during the polymerization process. The other saturator was used to saturate a He stream with bromoethane for the “in situ” quaternization process. (b) A reaction chamber, where the plasma condition

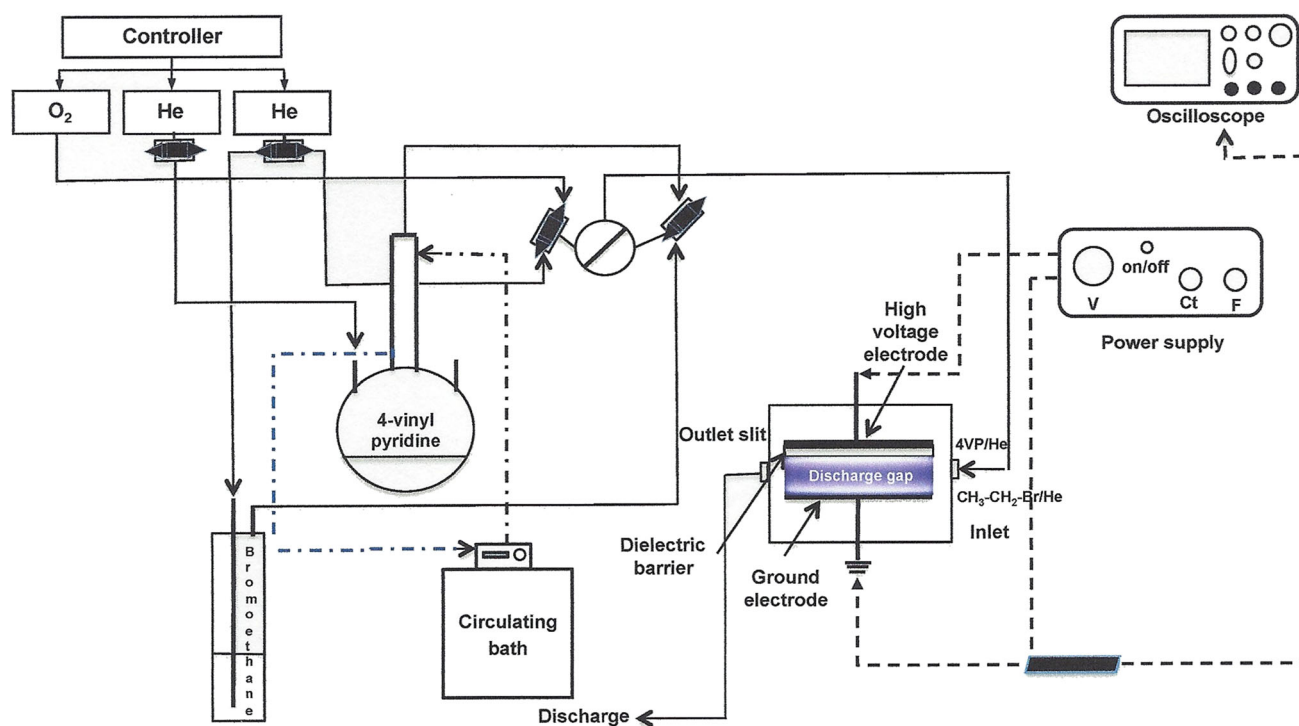


Figure 1 Schematic representation of the experimental system used for sequential polymerization of 4VP and quaternization of P4VPX films.

was generated. This chamber was constructed with Nylamid. Two circular 9-cm plates were used as electrodes. One of the electrodes was made of copper, and it was covered with commercial glass (acting as a dielectric barrier); the other electrode was made of stainless steel and had no glass cover. The space between the two electrodes, known as interelectrode distance, was set at 1 mm. The system also included a high-voltage, AC pulsed power supply, which regulated the input voltage to the power supply, the frequency (f), and the duty cycle (dc); these parameters determined the characteristics of the plasma condition in the chamber, which was used to activate the PE surface prior to the polymerization process.

Formation of polymer films

P4VP and P4VPQ films were made in a sequential gas-phase process at atmospheric pressure and room temperature. Figure 2 illustrates the main steps in this process. Initially, a circular PE sample with a diameter of 8.5 cm was placed at the center of the stainless steel electrode. Then, an O₂ plasma pretreatment was made to clean the sample and to end up with a more uniform PE surface. The O₂ plasma

was generated in the reaction chamber by flowing 100 ccm of O₂ and using the following parameters for the power supply: $f = 1667$ Hz and $dc = 10\%$. The plasma treatment was held for 5 min. Afterward, the chamber was purged with a 100 ccm He stream for 3 min.

The P4VP structure was sequentially formed in several cycles. For each cycle, a He plasma was used to generate free radicals, which chemically activate the PE surface. He plasma condition was obtained by flowing 100 ccm of He and setting the power supply at $f = 1667$ Hz and $dc = 10\%$; these settings produced a peak-to-peak voltage of about 45 kV. He plasma treatment time was 5 min. After the He plasma condition was stopped, 100 ccm of He saturated with 4VP at room temperature was fed to the reactor during 5 min; under this condition, the polymerization of 4VP was induced by a free radical mechanism. Next, the plasma chamber was purged with 100 ccm of He during 5 min to remove the gaseous residues from the polymerization step. In this work, we evaluated the effect of the number of treatment cycles, 4, 6, or 12 cycles on the resulting properties of P4VP films. These samples were labeled as P4VPX, where X is the number of treatment cycles.

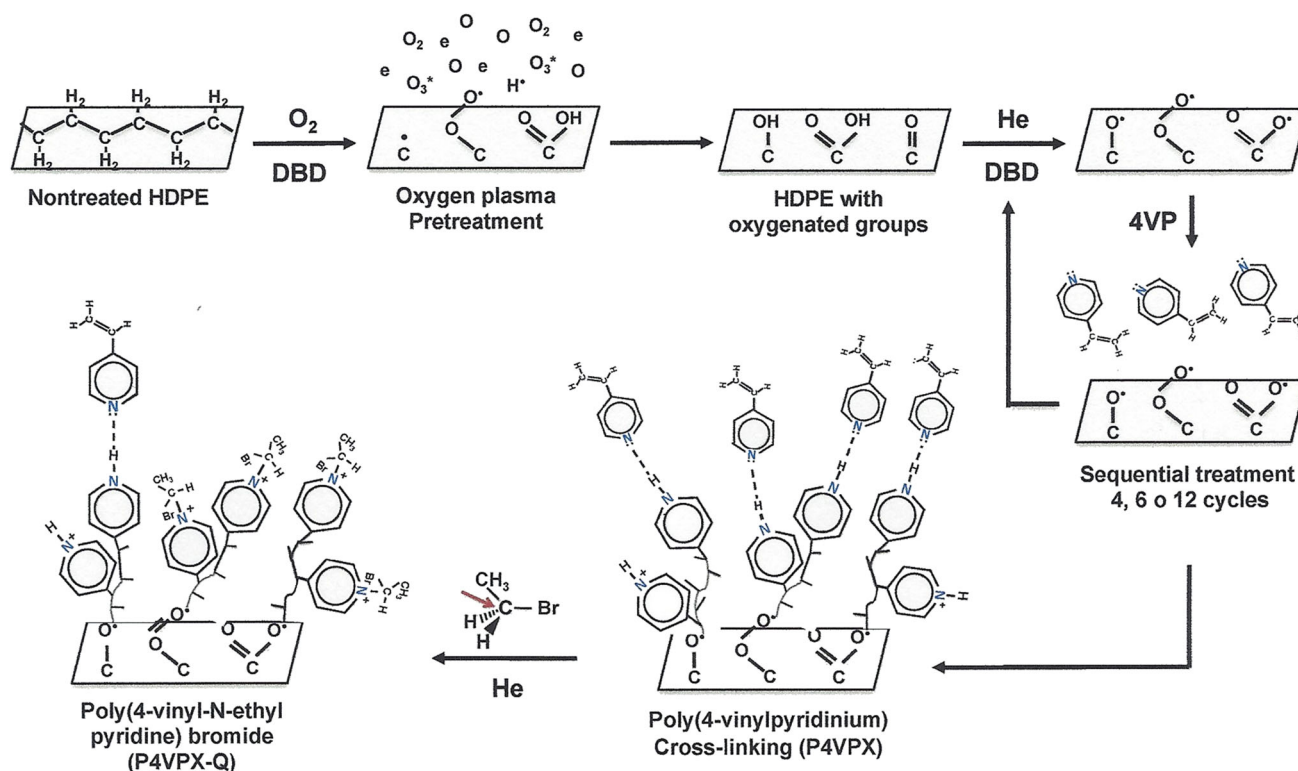


Figure 2 Schematic representation of the experimental sequence used for the synthesis of P4VPX and P4VPX-Q films.

After completing the selected number of cycles in the polymerization step, the in situ film quaternization of the P4VP films was carried out immediately in the same chamber. To this purpose, a 50 ccm He stream saturated with ethyl bromide at room temperature was used. Ethyl bromide has high reactivity, and its simple structure avoids the formation of bulky groups that typically decrease the process kinetics [14]. In addition, ethyl bromide has a high vapor pressure at the conditions of the experiment ($P_{\text{v bromoethane}}$ at 25 °C = 614 mmHg). The stream of He saturated with ethyl bromide was flown to the reactor during 60 min. The quaternized samples were labeled as P4VPX-Q.

Morphological characterization of polymer films

Surface texture of PE, P4VPX, and P4VPX-Q films was evaluated by using an optical microscope from OLYMPUS (PME3 series). In this microscope, visible light was reflected to a digital camera and the microscopic image was taken in digital format using PixelLink software. All microphotographs were obtained with a 10× objective. In addition, surface microstructure of PE, P4VPX, and P4VPX-Q films

was evaluated with an atomic force microscope (AFM) from Bruker (Dimension Edge). Images of different sections of each sample were obtained in the tapping mode using silicon doped antimony tips (Veeco's RTESP model). Roughness analysis of AFM images was performed with images of 10 × 10 μm and 20 × 20 μm with Nanoscope software (v.1.40).

Chemical surface characterization of polymer films

Chemical surface characterization of PE, P4VPX, and P4VPX-Q films was performed through FTIR spectroscopy from Thermo Scientific (Nicolet 6700 model). Analyses were made with a horizontal ATR cell with diamond crystal (Smart Orbit Diamond Crystal). Identification of the surface functional groups was made by using the IR spectrum collected in the 4000–667 cm⁻¹ range, with a resolution of 4 cm⁻¹ and 128 scans. Supplementary chemical characterization of the films was done by evaluating the presence of surface functional groups acting as chromophores [15]. To this purpose, a Thermo Scientific UV–visible spectrophotometer (Genesys 10 UV) was used. The UV spectrum was obtained in the wavelength range of 200–800 nm.

Evaluation of antimicrobial efficiency of polymer films

The antimicrobial efficiency of the P4VPX and P4VPX-Q films was determined using a method reported by Chen et al. [16] and according to the Japanese Industrial Standard [17]. A strain of *E. coli* was used for this purpose. The bacterium was activated by dispersing it into a trypticase soy broth and incubated for 24 h at 35 ± 1 °C. Then, a sample of the broth was taken and streaked on trypticase soy agar surface and incubated for 24 h at 35 ± 1 °C. To prepare the inoculum, an *E. coli* colony was dispersed in a physiological saline phosphate buffer solution to achieve an equivalent concentration of 10^6 organisms/mL in the McFarland scale. Next, the following dilutions were prepared: 1×10^{-1} , 1×10^{-2} , 1×10^{-3} , 1×10^{-4} , 1×10^{-5} , and 1×10^{-6} . The number of cells was estimated with the plate count method; this technique was performed by placing 1 mL of the 1×10^{-5} and 1×10^{-6} dilutions in Petri dishes (per duplicate); then, trypticase soy agar was poured and the samples were incubated at 35 ± 1 °C for 24 h.

The bactericidal properties of P4VPX and P4VPX-Q films were evaluated according to the following procedure. 0.1 mL of 1×10^6 CFU/mL *E. coli* was transferred to a glass coverslip (24×50 mm), which was placed in a Petri dish. Then, a 1.35×3 cm sample of the 4VPX or P4VPX-Q film was placed on top of the coverslip, and both were poured into a Petri dish with 10 mL of 10% glycerol (to maintain the box humidified and to prevent the damage of bacteria by drying) and incubated at 35 ± 1 °C for 24 h. After this step, the coverslip with the polymer film was placed in a sterile plastic cup with 9.9 mL of a sterile physiological saline solution (phosphate buffer). The vessel was shaken for 1 min to detach the film coverslip; then, it was homogenized and 10^{-1} and 10^{-2} dilutions were made. Subsequently, 1 mL of these solutions was placed in Petri dishes where trypticase soy agar was poured; the system was incubated for 24 h at 35 ± 1 °C. Finally, the number of CFU was counted and recorded for each dilution. The antimicrobial efficiency was calculated from the average number of bacteria in the control and test samples.

Results and discussion

As indicated, synthesis of P4VPX films was performed in a sequential process using the “post-irradiation grafting” approach [2, 5]. The selection of a dc = 10% was consistent with previous reports indicating that a proportionally shorter ignition time (t_{on}) in pulsed plasmas offers a better alternative to induce free radical polymerization, leading to polymeric structures similar to those obtained by conventional polymerization methods [18]. Under the operating conditions used in this study, the ignition time of the power supply (t_{on}) was around 0.6 ms and the shut-down time (t_{off}) was 5.28 ms. Thus, there was a short time in which the reactive species from the He plasma (free radicals) were formed; these radicals interacted with the substrate surface to “activate” the sites required to promote polymerization when the stream of He saturated with 4VP was flown into the chamber. In this study, the previously described cycle was done in $X = 4, 6,$ or 12 times to improve the polymeric film thickness and, as a result, the number of sites where a surface charge could be developed. Finally, after the polymerization process, the P4VPX films were quaternized “in situ” by using a He stream saturated with ethyl bromide.

Pretreatment of PE with oxygen plasma

PE pretreatment with O_2 plasma was performed to promote better adhesion of the polymeric film to the substrate. The extent and uniformity of the O_2 plasma treatment were evaluated by measuring the contact angle and the isoelectric point (IEP) of the oxidized PE surface. With respect to the first measurement, it was found that the contact angle on the PE surface decreased from 87° to 53° after the O_2 plasma treatment; this result was explained in terms of the formation of oxygenated surface groups, which increased the surface hydrophilicity. In the case of the second measurement, the zeta potential of the oxidized PE sample was measured as a function of pH to determine the IEP. It was found that the O_2 plasma treatment decreased the IEP from 3.65 to 3.2, which was also in agreement with the formation of oxygenated surface groups with acid character. The results just described were very similar for different PE samples used in this work, indicating that the O_2 plasma pretreatment was adequate to generate a

uniform condition for the PE samples prior to the polymerization process.

P4VP film formation on PE

As indicated, the P4VP film was formed in a cycle involving the exposure of oxidized PE surface to the free radicals generated in He plasma; this condition activates the surface and induces the 4VP polymerization process. This cycle was repeated 4, 6, and 12 times to generate samples P4VP4, P4VP6, and P4VP12, respectively. The samples were then characterized to validate the formation of the P4VP structure by spectroscopy techniques and the morphology (uniformity and thickness) of the polymer film by microscopic techniques.

Figure 3 shows the ATR infrared spectra for the samples P4VP4, P4VP6, and P4VP12, as well as the spectrum corresponding to a sample of P4VP with a molecular weight of 160,000, which was used as standard. In general, the IR vibration bands found in the spectrum were due to PE and 4PVP. Bands of greater intensity were located at 2913 and 2844 cm^{-1} ; these IR bands were associated, respectively, to the asymmetric and the symmetric stretching of the C-H bond in the PE methylene groups [19]. Other characteristic substrate IR bands were a doublet at 1475 cm^{-1} , corresponding to the methylene deformation, and a doublet around 730 cm^{-1} , which was related to the stretching of a C-H bond in the hydrocarbon chain. On the other hand, the IR

absorption bands characteristic of P4VP were also identified (Fig. 3). The broad band between 3340 and 3500 cm^{-1} was caused by stretching of a secondary amine NH and hydrogen bonds [13, 19]. The vibration band at 1637 cm^{-1} indicated the protonation of nitrogen of the pyridine group [20]. Moreover, the IR bands located at 1601, 1547, and 1407 cm^{-1} were associated with pyridine stretch modes [21]. The IR band at 1370 cm^{-1} was related to the symmetric bending vibration of C-H bond in a methyl group (CH_3 -) and the band at 1338 cm^{-1} to vibrations of methylene groups [22]. Furthermore, the IR band at 1232 cm^{-1} was associated with C-N stretching of the aromatic ring and IR bands located between 1000 and 700 cm^{-1} (856 and 825 cm^{-1}) were assigned to C-H bending vibrations outside the ring's plane [19]. Finally, a thin vibration around 1701 cm^{-1} could be due to C=O stretching, C=O ketones, aldehydes, esters, and carboxylic acids [19], which could be generated during the O_2 plasma treatment. Comparison of the spectra shown in Fig. 3 indicated that an increase in the number of treatment cycles from 4 to 12 reduced the intensity of the PE bands and increased the intensity of the distinctive P4VP bands. In more detail, P4VP12 exhibited a stronger wide-band between 3500 and 3340 cm^{-1} due to the NH stretching and also stronger bands at 1637 and 1601 cm^{-1} that were due to nitrogen protonation and pyridine stretching, respectively. These results reveal that the experimental approach used in this work favored the formation of P4VP films on PE. In addition, it was shown that a greater number of cycles (12) produced a polymeric film with a better definition of the IR bands distinctive of P4VP. Thus, it was initially associated with the formation of a thicker film and/or better uniformity of the polymeric surface.

On the other hand, Fig. 4 includes the UV-visible absorption spectra of the samples P4VP4, P4VP6, and P4VP12, as well as the P4VP sample used as reference. Figure 4a shows two well-defined UV bands, one strong band at 206 nm and one weak band at 258 nm. According to the literature, these bands were associated with $n \rightarrow \pi^*$ transitions of N atoms with unshared electron pairs [15]. Figure 4b shows that P4VP exhibited the two indicated UV bands. However, in the first case, a notorious shift from 206 to 232 nm was observed; this shift was associated with a bathochromic effect that occurs when the absorption wavelength shifts to longer wavelengths, indicating the formation of the pyridine cation [15]. In the

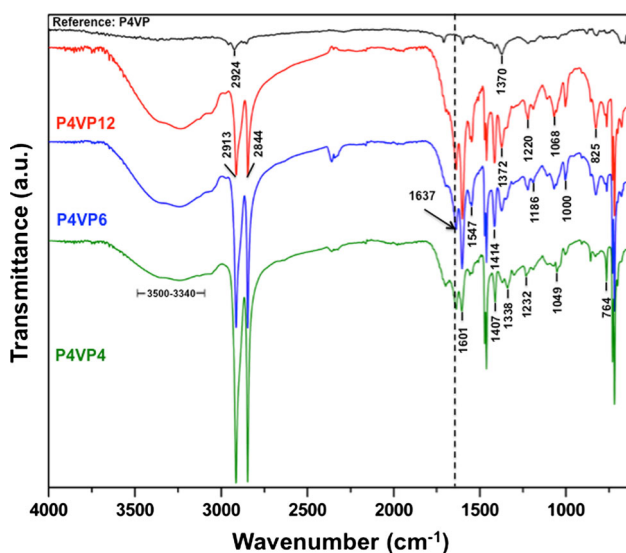


Figure 3 ATR spectra of a P4VP used as reference; b P4VP12; c P4VP6; d P4VP4.

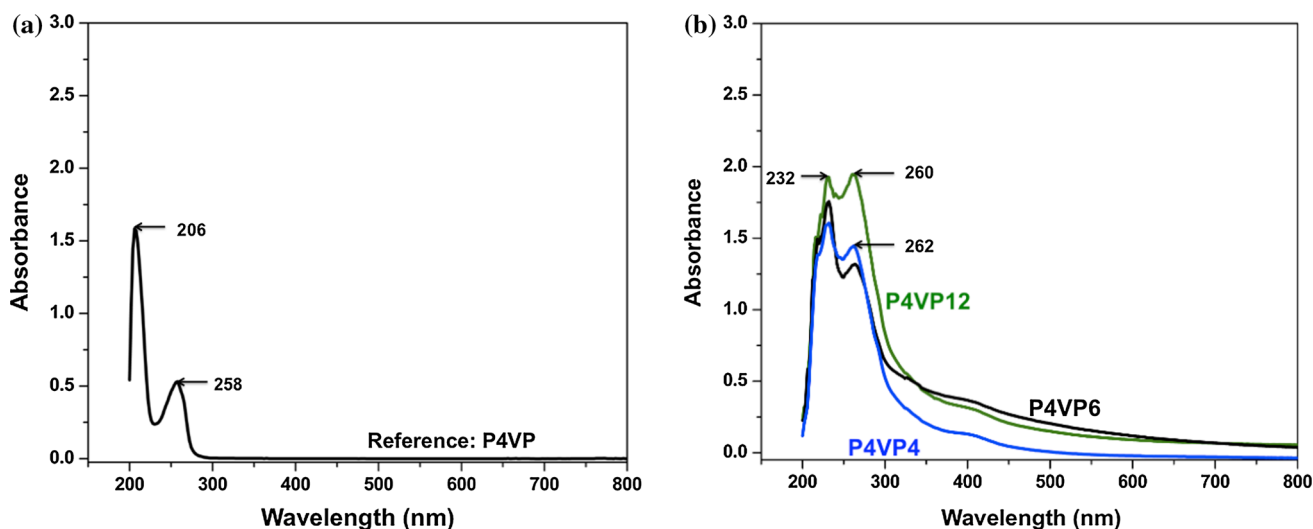


Figure 4 UV-Vis spectra of P4VP: **a** used as reference and **b** P4VP4, P4VP6 and P4VP12 films.

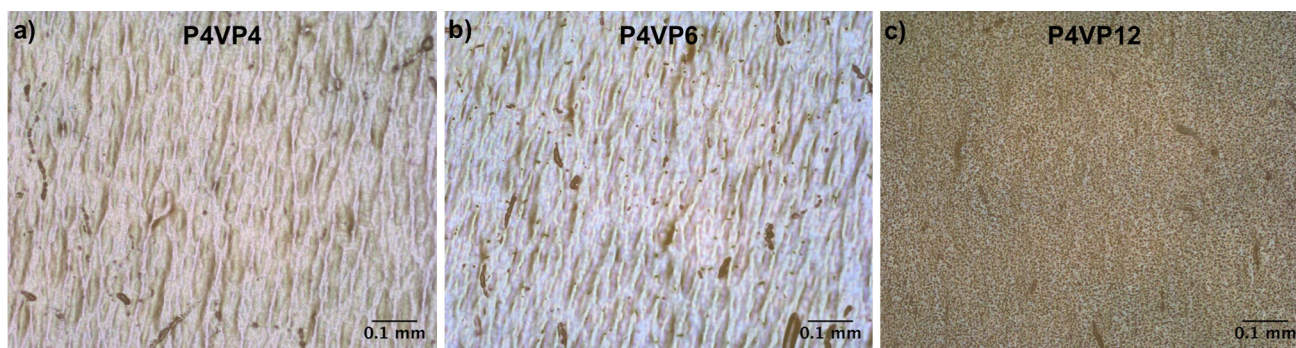


Figure 5 Optical photomicrograph of **a** P4VP4; **b** P4VP6; **c** P4VP12.

second case, a slight shift from 258 to 262 nm was found, suggesting that the aromatic ring of pyridine did not undergo significant changes. It should be noticed that the intensity ratio of the characteristic bands for each sample was notoriously different. In the case of the P4VP reference, the band intensity at 206 nm to the band at 258 nm (I_{206}/I_{258}) was about 3 units. However, the I_{232}/I_{262} ratio for P4VP-X films was markedly decreased with respect to the P4VP standard, and it also decreased when the number of cycles increased from 4 to 12.

Figure 5 shows the optical photomicrographs for the P4VP-X samples. P4VP4 and P4VP6 samples exhibited birefringence, which was mainly due to the contributions of the crystalline PE region (refractive index of 1.5) and the amorphous P4VP film region (refractive index of 1.57 at 532 nm) [23], was also observed. In contrast, the photomicrograph of P4VP-12 showed to be much more homogeneous in

morphological terms. Therefore, it was postulated that the conditions used in the synthesis of P4VP-12 were suitable to achieve almost total PE coating.

Quaternization of the P4VP film with bromoethane

Quaternization of P4VP films was performed in situ, in the same chamber, in a sequential process right after polymerization. To this purpose, a He stream saturated with ethyl bromide at 25 °C was flown to the reactor to quaternize the pyridine nitrogen atoms in the P4VP-X samples. The surface structure of the quaternized samples (P4VPX-Q) was also characterized by infrared and UV-Vis spectroscopy, and the morphology of the films was evaluated with optical and atomic force microscopy.

Figure 6 shows the IR spectra obtained by ATR for P4VP4-Q (Fig. 6a), P4VP6-Q (Fig. 6b), and P4VP12-Q (Fig. 6c); in each case, the comparison with the

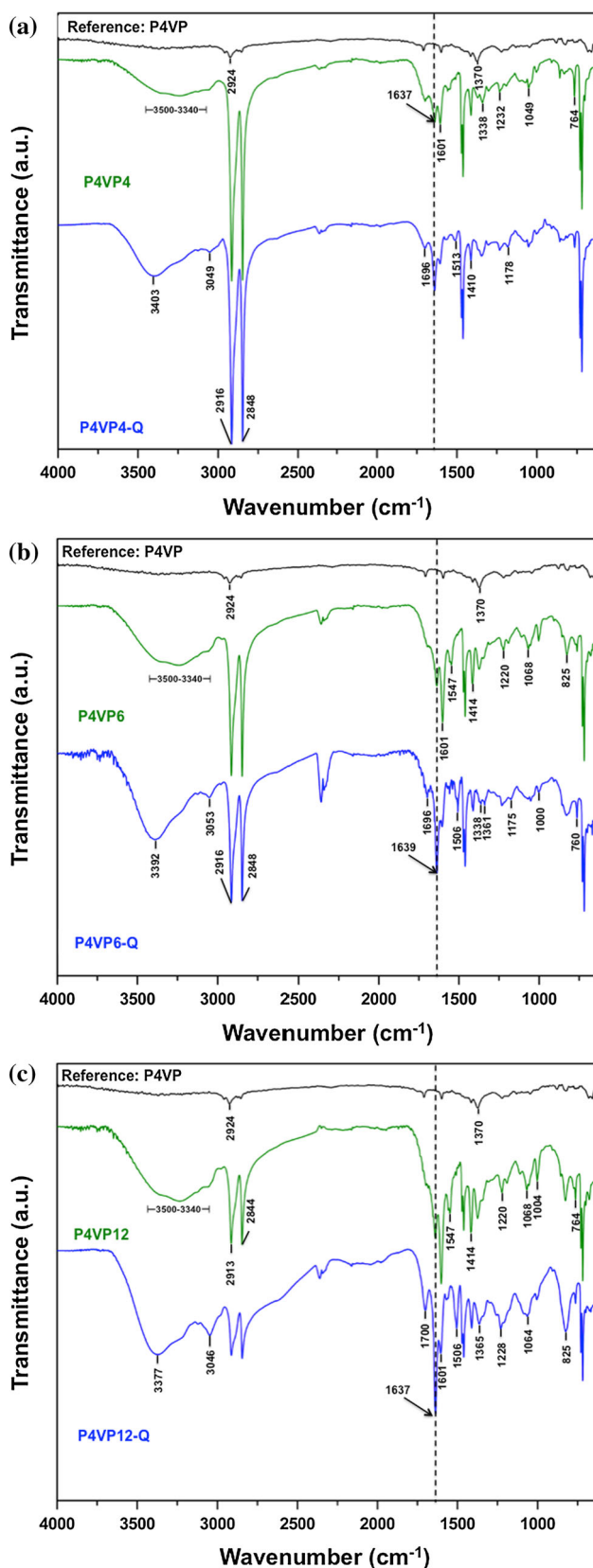
corresponding non-quaternized sample is also shown. P4VPX-Q samples still showed IR absorption bands due to PE and P4VP-X. The most distinctive IR absorption band after quaternization was the vibration band at 1637 cm^{-1} , which was associated with the protonation of the pyridine's nitrogen group [20]. Before the quaternization treatment, the intensity of this IR absorption band was similar for all polymeric films, independent of the number of polymerization cycles. After quaternization, the intensity of this band increased progressively from sample P4VP4-Q to samples P4VP6-Q and P4VP12-Q. In addition, a progressive decrease in the band around the 1601 cm^{-1} band was observed; this band is characteristic of the stretching of the pyridine's aromatic ring [21]. Another striking feature of the ATR spectrum of P4VPX-Q samples was the increase in an absorption band around $3377\text{--}3403\text{ cm}^{-1}$ due to the stretching of a secondary NH amine [19].

Figure 7 shows the absorption UV-visible spectra of P4VP4-Q (Fig. 7a), P4VP6-Q (Fig. 7b), and P4VP12-Q (Fig. 7c), including the comparison with the respective spectra of the un-quaternized samples. For P4VP4-Q, a shift in the absorption bands with respect to the P4VP4 was found. More specifically, the band associated with the formation of the pyridine cation (232 nm) was shifted to 252 nm; similarly, the absorption band assigned to the pyridine's aromatic ring (262 nm) was shifted to 288 nm. For P4VP6-Q, Fig. 7b indicates the first absorption band was shifted from 232 to 248, and the second absorption band was shifted from 262 to 290 nm. For sample P4VP12-Q, the first absorption band shifted from 232 to 246 nm and there was practically no shift of the absorption band initially encountered at 260 nm. This result suggests that P4VP12-Q still had a high concentration of pyridine nitrogen without quaternization.

Figure 8 shows the optical microphotographs of the P4VPX-Q samples. Similarly to the P-4VPX samples, P4VP4-Q and P4VP6-Q exhibited birefringence and the sample P4VP12-Q was more morphologically homogeneous. Thus, optical microscopy showed no appreciable change in morphology due to the quaternization process. Additionally, Fig. 9 includes micrographs obtained by AFM for P4VPX and P4VPX-Q samples. Figure 9a shows that roughness of sample P4VP-4 (R_{rms} (Rq) of $37 \pm 5\text{ nm}$) decreased after quaternization treatment (R_{rms} (Rq) $9 \pm 7\text{ nm}$). The amplitude images of these two samples showed no significant difference, since the energy dissipation

was 1.4 and 0.9183 V for P4VP4 and P4VP4-Q, respectively. These results suggest that both films had the same surface hardness. Similarly, phase images showed no differences; the phase shift observed in the films surface was 57.9° and 49.4° for the samples before and after quaternization, respectively. Given the fact that AFM is sensitive to the interatomic repulsion force that occurs between the tip and the film surface [24], it may be assumed that the cationic charge density and the degree of cross-linking on the surfaces of P4VP4 and P4VP4Q were qualitatively similar. Figure 9b shows that the roughness and the energy dissipation of P4VP-6 varied with the quaternization process; R_{rms} (Rq) changed from $8 \pm 4\text{ nm}$ to $18 \pm 14\text{ nm}$, and energy dissipation shifted from 0.096 to 0.0883 V. Similarly, phase images indicated an increase from 5.8 to 10.7° in the phase shift during quaternization. In agreement with these results, it was postulated that the P4VP6 surface was harder than the P4VP6Q surface due to a greater degree of cross-linking in the P4VP6 sample. Similar results were also found when comparing the polymeric films obtained after 12 cycles before (P4VP12) and after quaternization (P4VP12Q). Figure 9c shows that R_{rms} (Rq) increased from 1 ± 1 to $11 \pm 3\text{ nm}$ and the energy dissipation from 0.033 to 0.148 V, suggesting that P4VP12 surface was harder than that of P4VP12Q.

To discriminate the mechanical difference among the phase images of P4VPX and P4VPX-Q samples, Fig. 10 shows the frequency in which the phase shift occurred in each sample. Figure 10a shows the distribution in samples P4VP4 and P4VP4-Q. Wide distributions were observed for both samples indicating a large mechanical response upon the action of the AFM tip. In sample P4VP4, a shoulder was also observed, which suggested the presence of two types of surfaces, probably the substrate and the polymeric film. Clearly, the difference between P4VPX and P4VPX-Q samples films diminished as the number of plasma cycles in the synthesis was increased. Figure 10b, corresponding to P4VP6 and P4VP6-Q films, showed that both distributions were narrowed and showed no shoulder. These distributions were centered around zero phase shift, indicating a harder film as a clear consequence of the reticulation produced by the plasma process. Finally, Fig. 10c shows almost the same distribution, suggesting identical mechanical properties for P4VP12 and P4VP12-Q films.



◀ **Figure 6** ATR spectra of P4VP used as reference, P4VPX and P4VPX-Q films for **a** $X = 4$; **b** $X = 6$; **c** $X = 12$ cycles.

Description of 4VP polymerization and P4VP quaternization processes

The characterization results described for P4VPX samples validate that the polymeric films were appropriately induced on the PE surface by the experimental approach used in this work. In more detail, the O_2 plasma treatment used in the first stage must have a beneficial effect to uniform the substrate surface and also to form oxygenated functional groups that promote the formation of the polymer film. The experimental sequence suggested for polymerization was consistent with the post-irradiation grafting process [5]. In this process, the substrate surface was activated in the first cycle by using He plasma, which favors the formation of free radicals. Then, the contact of the active surface species with a 4VP/He stream induces the reaction of free radicals with π electrons of the double bond of the 4VP molecule. The breaking of the vinyl group is homolytic, and the active site is anchored to the PE surface by a covalent bond. If it is assumed that there is only one active site, the polymeric chain grows uni-directionally on the PE surface. In the second cycle of the polymerization sequence, the procedure is similar. He plasma activates the surface functional groups of the PE substrate, and it also activates the polymer chains formed in the previous cycle creating free radicals that may bond to other free radicals on a different chain. These reactions lead to the cross-linking of the growing polymer. Thus, it can be postulated that the polymer chain growth and the polymer film thickness are a function of the number of cycles of the process described above.

Results of ATR suggested that hydrogen bonding took place during polymerization; this was shown by NH bonds of primary and secondary amines, which have stretching frequencies around $3420\text{--}3340\text{ cm}^{-1}$ [19]. Amines involved in hydrogen bonding can expand IR absorption, and as a result, one or more superimposed IR bands may be found in the broad absorption of the NH stretching [14]. In the quaternization process, the N atoms in the pyridine ring of P4VP act as a strong negatively charged nucleophile, and the carbon atom in ethyl bromide acts as an electrophilic agent because it is bonded to an

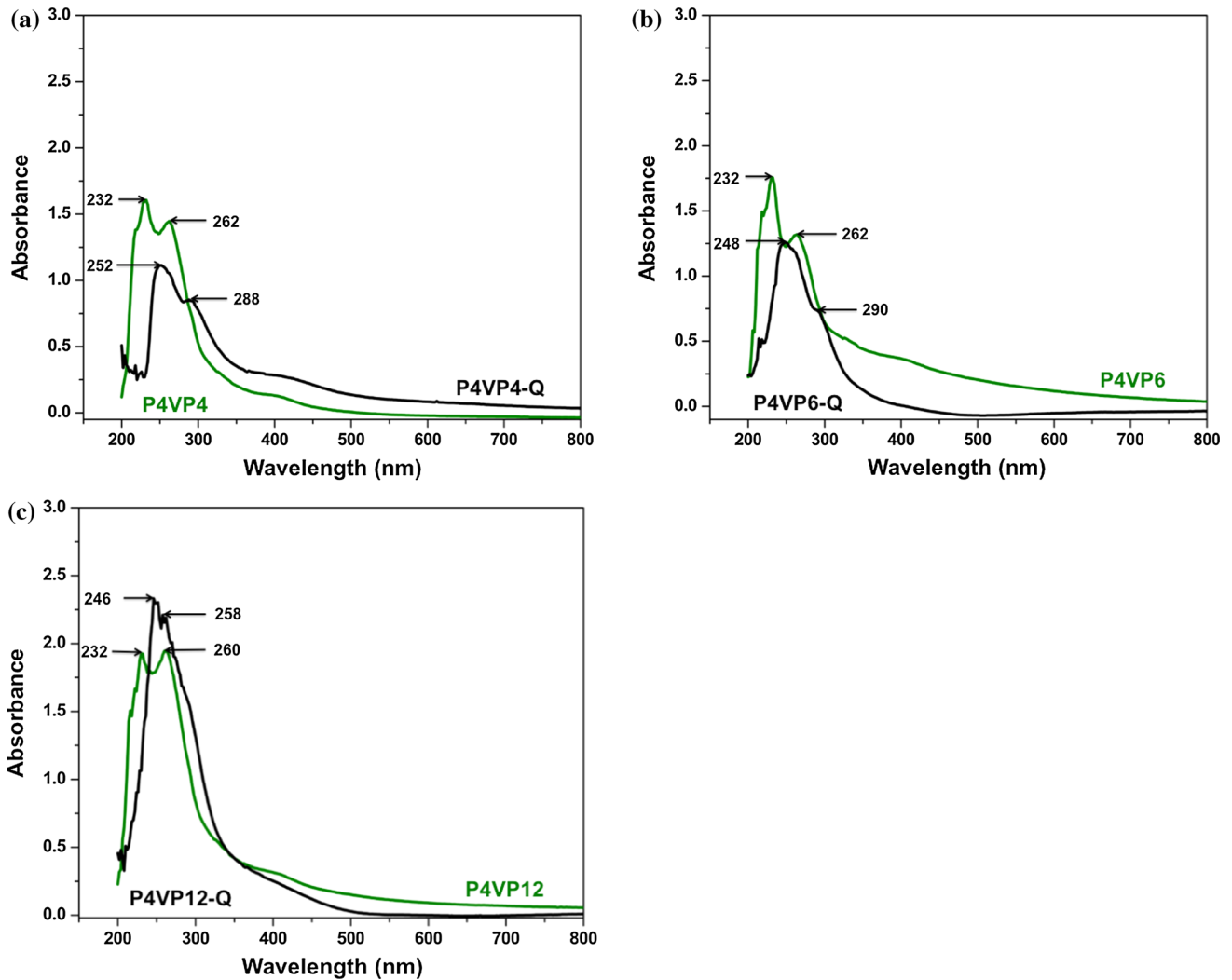


Figure 7 UV-Vis spectra of P4VPX and P4VPX-Q films for: **a** $X = 4$, **b** $X = 6$ and **c** $X = 12$.

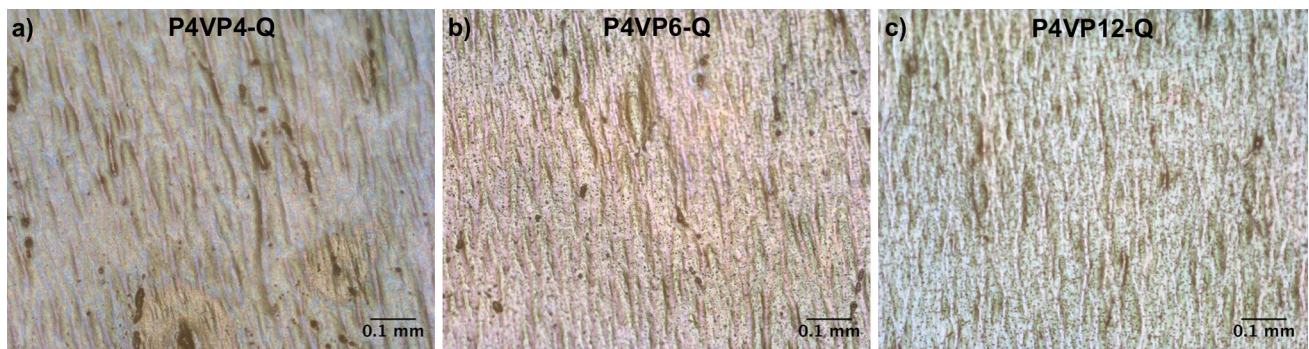


Figure 8 Optical photomicrographs of P4VP4-Q, P4VP6-Q, and P4VP12-Q films.

electronegative bromine atom and it exhibits a partial positive charge [14]. In this way, the negative charge of N atoms in the pyridine rings is attracted to the

positive charge of bromoethane carbon atoms to form a quaternary ammonium salt.

Thickness and charge density determination of P4VPX and P4VPX-Q films

The thickness of P4VPX and P4VPX-Q polymer films was obtained by scanning electron microscopy (SEM). Figure 11a, b shows 100,000-X micrographs of a cross section of P4VPX and P4VPX-Q films, respectively. In each of these figures, the arrow indicates the thickness of the polymer film. These results were analyzed with box diagrams, which are representative of the distribution of a data set built with five descriptive measures of the data; box diagrams provide information about the central tendency, dispersion, and symmetry of the data. Figure 12 shows that P4VPX film thickness linearly varied with the number of processing steps. It was also evident that films thickness increased with the quaternization process. The largest deviations of this trend were found in samples synthesized with 4 polymerization cycles. Deviations decreased for 6 and 12 cycles, for which optical microscopy and atomic force results showed greater morphological homogeneity (uniformity). Based on these results, P4VPX films thickness ranged from 122 to 307 nm and from 224 to 369 nm for P4VPX-Q films. With this information, a charge density was estimated for each polymeric films before and after quaternization.

Density (1.114 g/cm^3) and molecular weight (106,148 g/mol) of P4VP were taken into account to calculate the poly (4-vinylpyridinium) charge density. On the other hand, to calculate the charge density of bromide poly (4-vinyl-*N*-ethyl pyridinium), it was assumed that the density was the same as that of P4VP, and a molecular weight of 214.11 g/mol was used. Clearly, on the basis of this calculation, the films charge density was proportional to their thickness.

Bactericidal properties of P4VP and P4VP-Q films

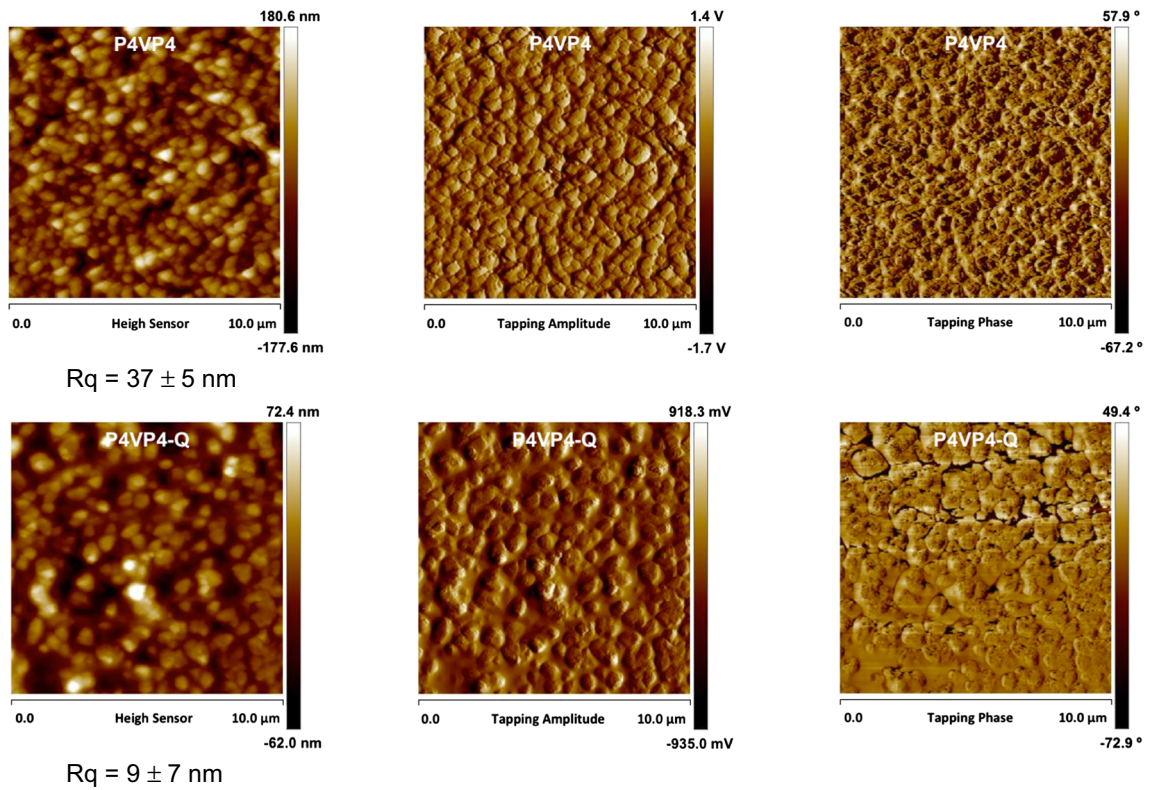
Figure 13 shows that when 0.1 ml of 1×10^6 CFU/ml of *E. coli* was placed in contact with a PE sample, 93,000 CFU/mL was found after 24-h incubation. This result indicates that PE had no bactericidal effect. Furthermore, Fig. 13 also shows that, under the same conditions, P4VP-4 and P4VP-6 films, with a charge density of 7.7×10^{16} and 1.3×10^{17} of N^+ atoms/ cm^2 , respectively, removed 95% of the *E. coli* bacteria. In addition, a sample of P4VP-12, with a

Figure 9 a AFM micrographs of P4VP4 (upper row) and P4VP4-Q (lower row) films. b AFM micrographs of P4VP6 (upper row) and P4VP6-Q (lower row) films. c AFM micrographs of P4VP12 (upper row) and P4VP12-Q (lower row) films.

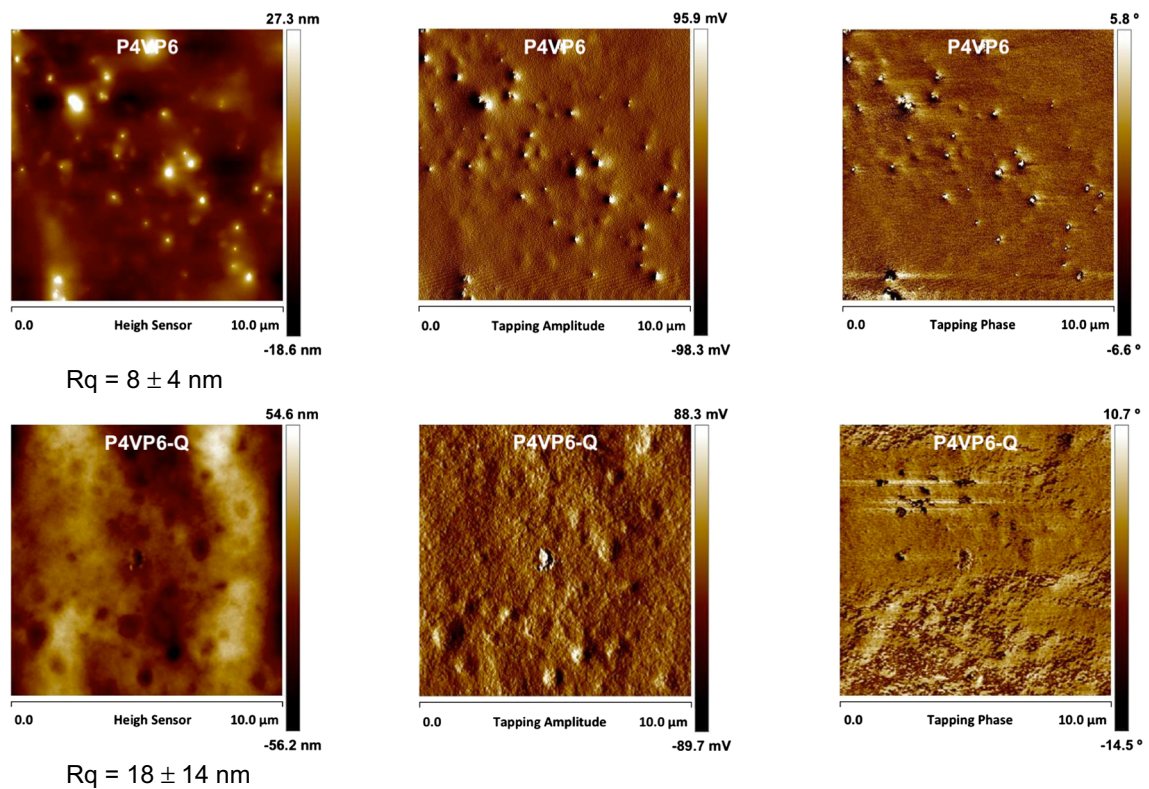
charge density of $1.9 \times 10^{17} \text{ N}^+$ atoms/ cm^2 , removed 99% of *E. coli* bacteria. On the other hand, P4VP4-Q, P4VP6-Q, and P4VP12-Q films, with a charge density of 7.0×10^{16} , 8.1×10^{16} , and $1.1 \times 10^{17} \text{ N}^+$ atoms/ cm^2 , respectively, were able to remove 99.96, 100, and 100% of *E. coli* bacteria. These results clearly indicate that the P4VP films synthesized in this work, by using a sequential approach including a free radical polymerization induced by dielectric barrier discharge process followed by an in situ quaternization of the polymer film, have a high bactericidal efficiency for a Gram-negative bacterium (*E. coli*). It is noted that the key factor for the bactericidal properties exhibited for both types of films was a high surface charge density.

Possible bactericide mechanisms of P4VP and P4VP-Q films

Several mechanisms have been proposed in the literature to explain the bactericidal effect of P4VP and P4VP-C films. One mechanism suggests that the surface of these films exerts electrostatic interactions with the bacterial anionic surface components; these interactions destabilize the outer membrane and promote the destruction of the bacterium. Kugler et al. [10] reported a high bactericidal efficiency of PVP-Q films with a charge density of $1.5 \times 10^{15} \text{ N}^+$ cm^{-2} for *E. coli* and $1.7 \times 10^{16} \text{ N}^+$ cm^{-2} for *S. epidermidis*. Their results showed that a minimum surface charge density is required to induce instant death and also that this minimum surface charge depends on the bacterial metabolism. Hong and Brown [25] indicated that the nature of the surface charge has a significant effect on the pH of the cell's surface and affects the ATP levels of the bacterium. They suggested that as the *E. coli* surface is close to a positively charged polymeric film, the local pH near the cell's surface increases in almost 2 units, establishing a reverse pH gradient through the bacterial cell wall; this reduces the formation of ATP causing the cell's death (Fig. 14). Other studies suggested that the polymeric structures with positive surface charge displace the lipopolysaccharide's positively charged



(a)



(b)

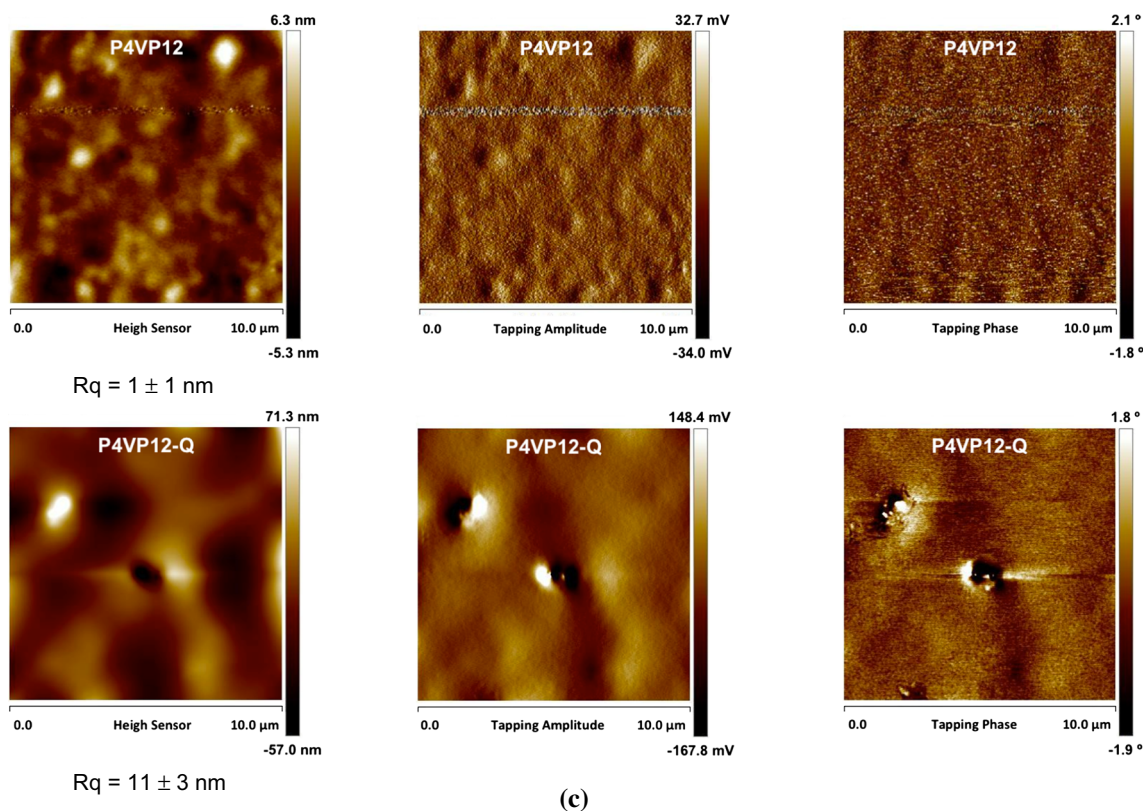


Figure 9 continued.

divalent cations (such as Ca^{2+} and Mg^{2+}) of a Gram-negative bacterium. These cations displacement is promoted on surfaces with a charge density equal or greater than the bacteria's surface charge density, which is 10^{14} to $5 \times 10^{15} \text{ N}^+/\text{cm}^2$, as a function of the cell growth stage. It is clear that the loss of the bacterium's structural cations results in the damage of the membrane's integrity [9, 10, 26, 27].

Another mechanism that prevents the growth of bacteria on the surface of P4VP-C films is attributed to the polymer structure. It is known that the antibacterial activity of pyridinium polymers is related to polymer properties, such as length, flexibility, and hydrophobicity/hydrophilicity of the alkyl pyridinium end. Tiller et al. [9] reported that polymers with C_3 to C_6 alkyl substituents have higher bactericidal activity than polymers with shorter (C_1 and C_2) or longer (C_7 – C_{16}) substituents. In contrast, Sambhy et al. [28] indicated that pyridinium polymers with short alkyl chains (C_1) had more bactericidal potential than polymers with longer alkyl chains (C_3 – C_5). Thus, there is no agreement of the effect of the structure on the bactericidal properties of P4VP-Q films. Murata et al. [27] suggested that

although soluble compounds can penetrate the cell's wall, molecules bound to the cell's surface are limited by their molecular length and they only penetrate the cell's membrane if they extend away enough from the cell's surface. Furthermore, these authors showed that the short chains with high grafting density and long chains with low grafting density were equally effective against *E. coli*.

Based on the bactericidal mechanisms proposed in the literature and results of characterization and bactericidal evaluation of P4VP and P4VP-Q films synthesized in this work, it is postulated that the interaction of P4VP and P4VP-Q films with the *E. coli* surface is mostly due to an electrostatic effect caused by the high surface charge density exhibited by both types of films (7×10^{16} to 1.9×10^{17}), which is higher than the surface charge previously reported in the literature for similar polymeric films.

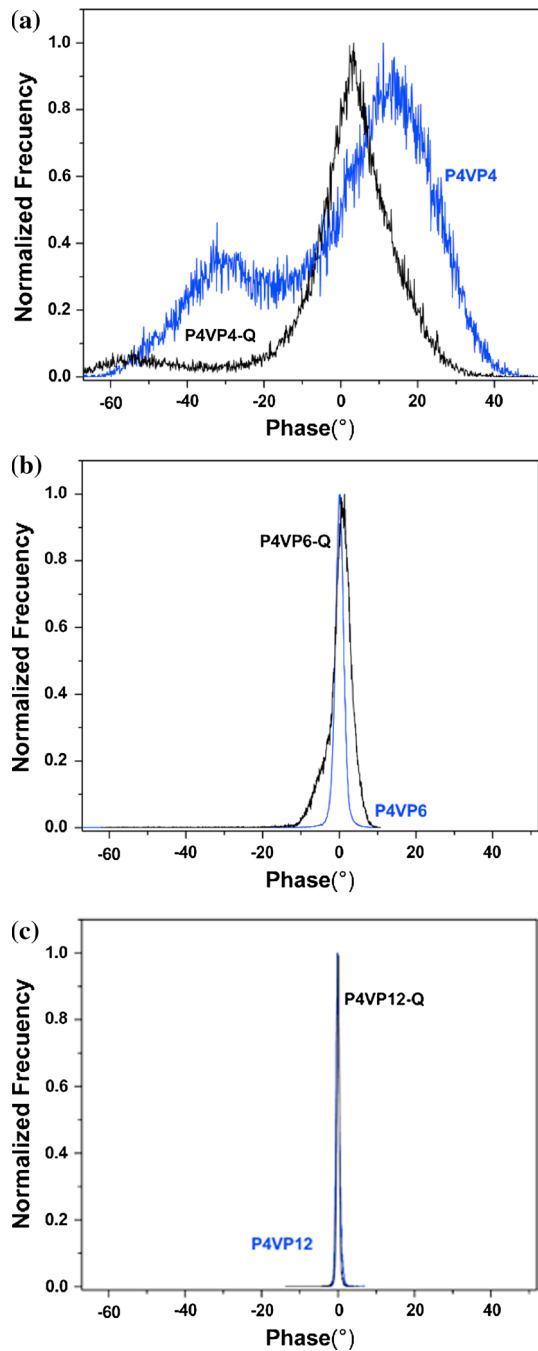


Figure 10 Phase angle distribution in P4VPX and P4VPX-Q films; **a** $X = 4$, **b** $X = 6$; **c** $X = 12$ cycles.

Evaluation of the proposed experimental sequence

To highlight the advantages of the experimental sequence developed in this work, we briefly reviewed the experimental approaches previously suggested in the literature for the synthesis of

quaternized 4PVP films with bactericidal properties. Tiller et al. [9] reported the synthesis of poly (4-vinyl-*N*-alkylpyridinium bromide) films supported on glass slides with surface groups densities from $0.4 \pm 0.05 \mu\text{g}/\text{cm}^2$ ($4.7 \times 10^{12} \text{ N}^+ \text{ cm}^{-2}$) to $5.8 \pm 3.0 \mu\text{g}/\text{cm}^2$ ($2.1 \times 10^{14} \text{ N}^+ \text{ cm}^{-2}$), as a function of the experimental sequence and the molecular weight of the monomer used in the synthesis. In a standard bactericidal test, the films synthesized by these authors eliminated $94 \pm 4\%$ of *Staphylococcus aureus* cells. In another work, Cen et al. [29] used polyethylene terephthalate (PET) and commercial paper filter as substrates to develop bactericide polycationic groups. Both substrates were initially pretreated with an Ar plasma followed by a UV-induced polymerization process of 4VP. In a subsequent set process, the pyridine surface groups were alkylated with hexyl bromide to produce the pyridinium groups. These authors reported the bactericidal properties of the quaternized polymeric films to eliminate *E. coli*, and they also indicated that a surface group density of $15 \text{ nmol}/\text{cm}^2$ ($9 \times 10^{15} \text{ N}^+ \text{ cm}^{-2}$) or greater was highly effective to remove *E. coli* adhered on the functionalized surfaces. Moreover, Kugler et al. [10] reported the synthesis of quaternized P4VP films on a glass substrate by two different approaches (“grafting from” and “grafting to”); the films developed a charge density between 10^{12} and 10^{16} positive charges per cm^2 , and their efficiency in bacterial mortality was a function of the metabolic state of the bacteria. For *E. coli* and *Staphylococcus epidermidis* under a low cell division condition, a charge density of $10^{14} \text{ N}^+ \text{ cm}^{-2}$ was required to have significant bactericidal properties. Under high cell division conditions, a lower charge density of 10^{12} and $10^{13} \text{ N}^+ \text{ cm}^{-2}$ was required for *E. coli* and *S. epidermidis*, respectively. In another work, Jiang et al. [13] reported 4VP polymerization on PET substrates by using AC pulsed plasma. After the polymerization, the film was placed in a silver nitrate solution and exposed to UV irradiation to promote the dispersion of silver nanoparticles on the P4VP film. The authors found that the resulting composite film showed bactericidal properties for *Delaromyces hansenii* and *Penicillium nalgiovense*; they also found that the antimicrobial properties were proportional to the thickness of the P4VP coating and the UV irradiation time, related to the dispersion of the silver particles in the composite film. Murata et al. [27] developed polymeric brushes with antimicrobial activity by radical polymerization

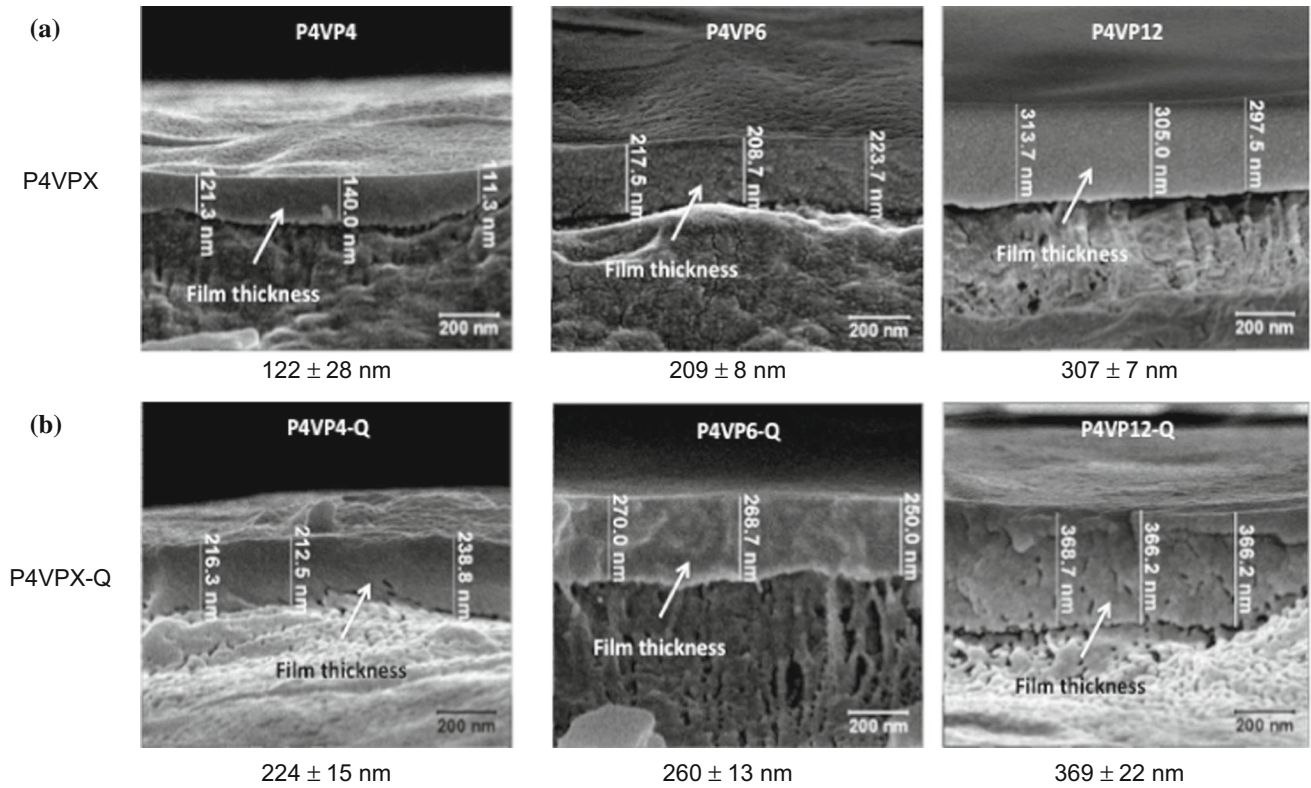


Figure 11 SEM micrographs obtained with $\times 100,000$. The arrow tip points the thickness of the P4VPX (upper row) and P4VPX-Q (lower row) films: **a** $X = 4$, **b** $X = 6$ and **c** $X = 12$ cycles.

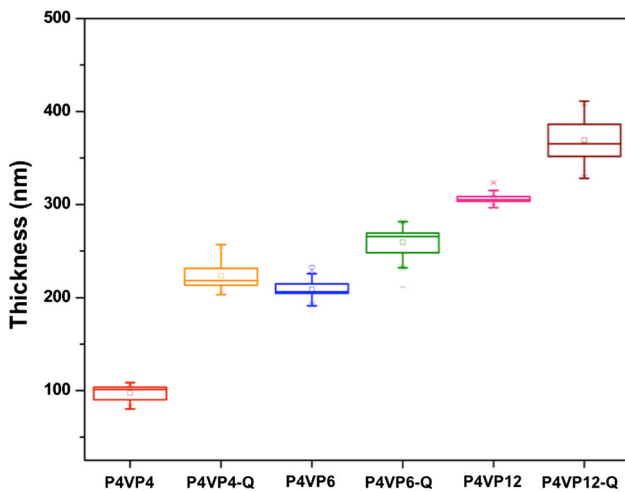


Figure 12 Box diagram of P4VPX and P4VPX-Q films.

of 2-(dimethylamino) ethyl methacrylate followed by quaternization of the amino groups with alkyl bromides. These authors also agreed that surface charge density is the key factor to obtain films with bactericidal properties and that a minimum surface charge density of $1\text{--}5 \times 10^{15}$ units of quaternary amines/ cm^2 is required on a film to exhibit bactericidal

properties. Moreover, Jampala et al. [11] used low-pressure ethylenediamine plasma to generate polymeric films with quaternary amino groups on stainless steel and filter paper. These authors reported that the surface polymeric structures and the bactericidal efficiency for *Staphylococcus aureus* and *Klebsiella pneumoniae* (higher than 96.8%) were very similar for the polymeric films regardless of the support. Furthermore, Schofield and Badyal [12] reported the synthesis of P4VP films on polypropylene and silicon wafers by using pulsed radiofrequency plasma at 13.56 MHz; the polymeric films were later quaternized with bromobutane. The bactericidal efficiency of the quaternized polymeric films for *S. aureus* (Gram positive) and *K. pneumoniae* (Gram negative) was practically 100%.

Based on the former information, the experimental sequence proposed in this work for the synthesis of P4VPX and P4VPX-Q films on commercial HDPE displayed some significant differences. First, the P4VPX films were obtained by a plasma syn-radiation approach. In this way, an O_2 plasma treatment was initially used to clean and to activate the HDPE

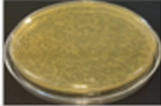

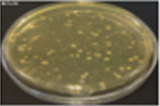
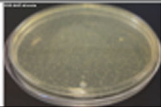
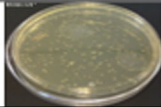

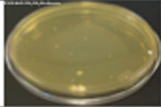

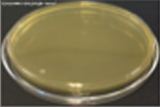



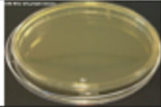
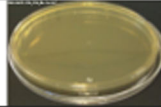
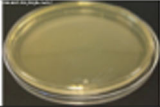
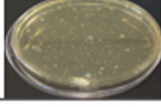
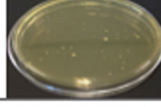
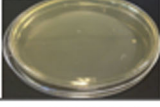
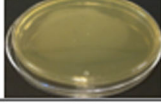
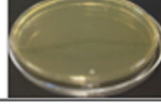

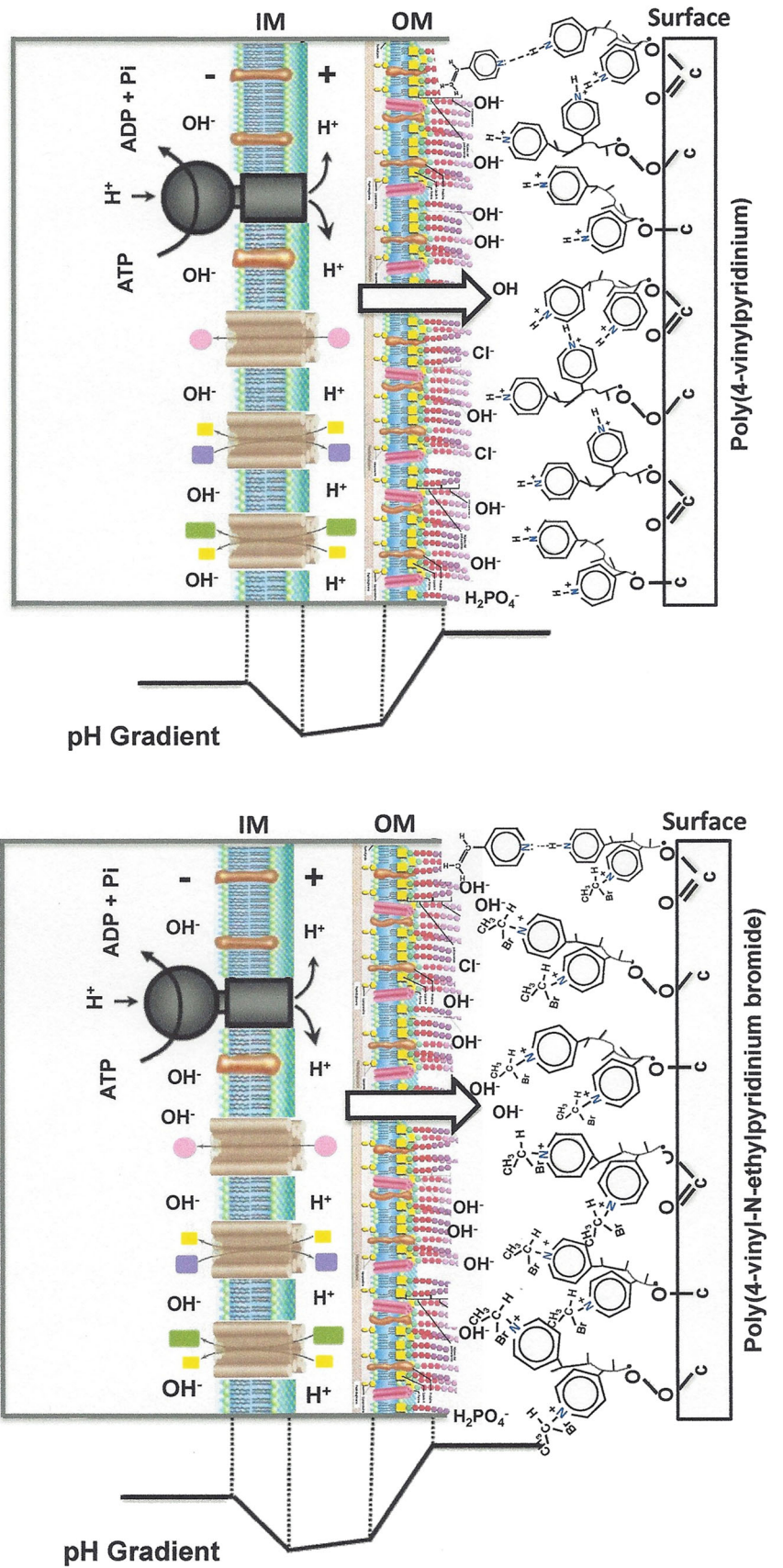
Treatment	Dilution without	10 ⁻¹	10 ⁻²	Antibacterial ratio
Untreated HDPE				
	Countless CFU/ml	Countless CFU/ml	< 250 CFU/ml	
P4VP4				94.78 ± 3.5%
	Countless CFU/ml	< 250 CFU/ml	49 ~ 4,900 CFU/ml	
P4VP4-C				99.96 ± 9%
	36 CFU/ml	4 ~ 40 CFU/ml	0 CFU/ml	
P4VP6				95.32 ± 3.5%
	Countless CFU/ml	< 250 CFU/ml	44 ~ 4,400 CFU/ml	
P4VP6-C				100%
	0 CFU/ml	0 CFU/ml	0 CFU/ml	
P4VP12				99.25 ± 4%
	< 250 CFU/ml	69 ~ 690 CFU/ml	5 ~ 500 CFU/ml	
P4VP12-C				100%
	0 CFU/ml	0 CFU/ml	0 CFU/ml	

Figure 13 Antimicrobial effect against *E. coli* of HDPE, P4VPX and P4VPX-Q films.

surface. Afterward, the polymerization of 4VP was carried out by using a cycle involving the generation of surface free radicals (under a He plasma condition) and then contacting the activated surface with the 4VP monomers in gas (with no plasma condition). It was shown that the P4VPX films thickness linearly varied with the number of polymerization cycles (from 122 to 307 nm) and also that the quaternization process further increased the films thickness (from 224 to 369 nm). For this reason, the estimated density of positive charges for the P4VPX and P4VPX-Q films obtained in this work (7.0×10^{16} to 1.9×10^{17} N⁺ atoms/cm²) was significantly larger than those reported in the literature. This observation was in agreement with the fact that both 4PVPX and 4PVPX-Q films exhibited high antibacterial activity for *E. Coli*. Previous reports in the literature suggested

that a positively charged polymer coating by itself was not sufficiently active to kill or inactivate the bacteria, thus requiring the alkylation of the polymer film to produce surface quaternary ammonium compounds with higher bacterial activity [7, 9, 11, 12]. However, the experimental results shown in this work suggested that if a dense surface polymer coating is obtained, with an appropriate cross-linking, the polymer coating may exhibit by itself significant bactericidal activity. Therefore, it is assumed that the polymerization cycle proposed in this work promoted the formation of a denser, grafted polymer that has a composition more similar to that obtained by conventional polymerization processes. In addition, if the quaternization process is required, results of ATR in this work showed that the treatment of P4VPX films with a gas stream of He saturated with

Figure 14 Schematic representation of the effect of charge regulation between the cell and a positively charged surface of P4VPX and P4VPX-Q. Adapted from [25].



ethyl bromide at T_{room} and P_{atm} , right after the polymerization cycle, was sufficient to promote the formation of quaternary ammonium salts with further bactericidal potential for *E. coli*.

In this way, the alternative procedure proposed in this work clearly showed some advantages over the experimental sequences previously indicated for the synthesis of quaternized P4VP coatings [11–13]. In general, the suggested procedure took place only in gas phase at room temperature. Polymerization and quaternization steps took short contact times, and a limited use of the precursors was made in each process; in fact, the quaternization step was solvent-free. Under the conditions used herein, the method yielded denser polymeric films with a significant thickness, resulting in estimated charge densities higher than those reported in previous studies. Therefore, the procedure developed in this work allows the control the polymeric film thickness based on the number of polymerization cycles. In addition, the ease of implementation may facilitate the commercial scaling of the overall process. In summary, the suggested procedure showed technical, economic, and environmental benefits as compared with previous approaches reported in the literature.

Finally, the suggested experimental sequence may contribute to the development of new universal coatings, fulfilling the conditions indicated by Wei et al. [4] for this kind of coatings: (a) the existence of some interaction between the coating materials and the substrate surfaces, (b) the presences of lateral cross-linking, (c) the synthesis of a coating with the appropriate functionality or the possibility to be further functionalized. Moreover, the dense polymer films obtained in this work may also contribute to the coating stability. Additionally, the operating plasma conditions used in this work could be extrapolated for engineering antibacterial coatings in fields where bacterial attachment is of concern, such as food packaging and industrial and marine fouling [1].

Conclusions

The RDBD-PP treatment system built in this work was proven to be a suitable alternative for the synthesis of P4VP and P4VP-C films with a surface charge density of at least 10^{16} positive charges per cm^2 . Both types of polymeric films synthesized in this work were able to destabilize and destroy the

bacterium *E. coli*. It was found that the bactericidal properties of P4VP and P4VP-C films were mostly due to electrostatic interactions between the polymeric film surface and the cell's surface, because the surface charge density of the polymeric films synthesized in this work was higher than that previously reported for similar polymeric films. The main contribution of the experimental sequence proposed in this work for the synthesis of the P4VPX and P4VPX-Q films is that the 4VP polymerization and the P4VP quaternization steps take place in a sequentially gas-phase process in the same treatment system, which was operated at T_{room} and P_{atm} . The polymerization process took 20–60 min, as a function of the number of polymerization cycles, and the quaternization process was completed in 60 min with a regulated amount of the precursors, low energy input, and no additional processing steps required. Importantly, the process may facilitate the regulation of the polymer film's thickness and, as a result, of the surface charge density that is a key factor to develop bactericidal surfaces. Therefore, the methodology proposed in this work for the synthesis of polymer coating with bactericidal activity is simpler, faster, and more environmentally friendly than conventional approaches. In comparison with other plasma-based approaches, the operation at T_{room} and P_{atm} may have a significant effect on the economics and the ease of implementation of the process at commercial scale.

Acknowledgements

MHO thanks Consejo Nacional de Ciencia y Tecnología (CONACyT) scholarship 228888. The financial support of CONACyT (Grants 162651 and 252320) and UASLP (Grant C13-FRC-01-04-04) for the development of the project is greatly appreciated. The authors thank Rosa E. Delgado-Portales for supplying the *E. coli* 11775 strain, and Claudia Arellano del Rio, Maria de Lourdes González-González, Claudia Guadalupe Elías, Gladis Judith Labrada-Delgado and Maria Estela Nunez-Pastrana for technical support.

Compliance with ethical standards

Conflict of interest Authors declare no conflict of interest.

References

- [1] Sardella E, Palumbo F, Camporeale G, Favia P (2016) Non-equilibrium plasma processing for the preparation of antibacterial surfaces. *Materials* 9:515–538
- [2] Jacobs T, Morent R, De Geyter N, Dubruel P, Leys C (2012) Plasma surface modification of biomedical polymers: influence of cell-material interaction. *Plasma Chem Plasma Process* 32:1039–1073
- [3] Cloutier M, Mantovani D, Rosei F (2015) Antibacterial coatings: challenges, perspectives, and opportunities. *Trends Biotechnol* 33(11):637–652
- [4] Wei Q, Haag R (2015) Universal polymer coatings and their representative biomedical applications. *Mater Horiz* 2:567–577
- [5] Desmet T, Morent R, Geyter N, Leys C, Schacht E, Dubruel P (2009) Nonthermal plasma technology as a versatile polymeric biomaterials strategy for surface modification: a review. *Biomacromol* 10(9):2351–2378
- [6] Nikiforov A, Deng X, Xiong Q, Cvelbar U, De Geyter N, Morent R, Leys C (2016) Non-thermal plasma technology for the development of antimicrobial surfaces: a review. *J Phys D Appl Phys* 49:2004002
- [7] Vasilev K (2014) Nanoengineered plasma polymer films for biomaterial applications. *Plasma Chem Plasma Process* 334:538–545
- [8] Siedenbiedel F, Tiller JC (2012) Antimicrobial polymers in solution and on surfaces: overview and functional principles. *Polymers* 4:46–71
- [9] Tiller JC, Liao CJ, Lewis K, Klibanov AM (2001) Designing that kill bacteria on surface contact. *PNAS* 98(11):5981–5985
- [10] Kugler R, Bouloussa O, Rondelez F (2005) Evidence of a charge-density threshold for optimum efficiency of cationic biocidal surface. *Microbiology* 151:1341–1348
- [11] Jampala SN, Sarmadi M, Somers EB, Wong ACL, Denes FS (2008) Plasma enhanced synthesis of bactericidal quaternary ammonium thin layers on stainless steel and cellulose surfaces. *Langmuir* 24(16):8583–8591
- [12] Schofield WCE, Badyal JPS (2009) A substrate-independent approach for bactericidal surfaces. *ACS Appl Mater Interfaces* 1(12):2763–2767
- [13] Jiang J, Winther-Jensen B, Kjær MS (2006) Characterization of plasma-polymerized 4-vinyl pyridine on poly (ethylene terephthalate) film for anti-microbial properties. *Macromol Symp* 239:84–90
- [14] Wade LG (2013) *Organic chemistry*, 8th edn. Pearson Education, London
- [15] Skoog DA, Holler FJ, Crouch SR (2007) *Principles of instrumental analysis*, 6th edn. Thomson Brooks/Cole, Belmont
- [16] Chen Y, Zheng X, Xie Y, Ding Ch, Ruan H, Fan C (2008) Anti-bacterial and cytotoxic properties of plasma sprayed silver-container containing HA coatings. *J Mater Sci Mater Med* 19:3603–3609
- [17] JIS Z 2801 (2000) Test for antimicrobial products-antimicrobial activity and efficacy. Jpn Stand Assoc, Japan
- [18] D’Agostino R, Favia P, Oehr C, Wertheimer MR (2005) Low temperature plasma processing of materials: past, present and future. *Plasma Process Polym* 2:7–15
- [19] Smith BC (1999) *Infrared spectral interpretation: a systematic approach*, 1st edn. CRC Press, Boca Raton
- [20] Harnish B, Robinson JT, Pei Z, Ramström O, Yan M (2005) UV-cross-linked poly (vinylpyridine) thin films as reversibly responsive surfaces. *Chem Mater* 17:4092–4096
- [21] Mistry BD (2009) *A handbook of chemistry data spectroscopic (UV, IR, PMR, 13C NMR and mass spectroscopy)*, 2009th edn. Oxford Book Company, Jaipur
- [22] Derrick MR, Stulik D, Landry JM (1999) *Infrared spectroscopy in conservation science*. J. Paul Getty Trust, Los Angeles
- [23] Billmeyer FW (1984) *Polymer science*, 3rd edn. Wiley, New York
- [24] Friedbacher G, Bubert H (2011) *Surface and thin film analysis: a compendium of principles, instrumentation, and applications*, 2nd edn. Wiley, New York
- [25] Hong Y, Brown DG (2009) Alteration of bacterial surface electrostatic potential and pH upon adherence to a solid surface and impacts to cell bionergetics. *Biotechnol Bioeng* 105(5):965–972
- [26] Terada A, Yuasa A, Kushimoto T, Satoshi T, Katakai A, Tamada M (2006) Bacterial adhesion to and viability on surfaces positively charged polymer. *Microbiology* 152:3575–3583
- [27] Murata H, Koepsel RR, Matyjaszewski K, Russell AJ (2007) Permanent, non-leaching antimicrobial surfaces 2: how high density cationic kill bacterial cells surfaces. *Biomaterials* 28:4870–4879
- [28] Sambhy V, Eves D, Ewing A, Sen A (2007) Direct visualization of lipid membrane disruption by antibacterial pyridinium polymers in GUV model systems. *Polym Prepr Am Chem Soc Div Polym Chem* 48(1):676
- [29] Cen L, Neoh KG, Kang ET (2003) Surface functionalization technique for conferring antibacterial properties to polymeric and cellulosic surfaces. *Langmuir* 19:10295–10303